Influence of working gas pressure on the performance of W/Si multilayers*

WANG Fang-Fang(王芳芳)[1] ZHU Jing-Tao(朱京涛)[1] ZHONG Qi(钟奇)[1]
WANG Zhan-Shan(王占山)[1;1)] Philippe Jonnard[2] Karine Le Guen[2]
Jean-Michel André[2] Michel Fialin[3]

[1] Institute of Precision Optical Engineering, Department of Physics, Tongji University, Shanghai 200092, China
[2] Laboratoire Chimie Physique – Matière Rayonnement, UPMC Univ Paris 06, CNRS UMR 7614, 11 rue Pierre et Marie Curie, F-75231 Paris Cedex 05, France
[3] Centre CAMPARIS, CNRS UMR 7154, campus Jussieu, 4 place Jussieu, F-75254 Paris Cedex 05, France

Abstract: The effect of Ar pressure on the performance of W/Si multilayers is investigated. W/Si multilayers were deposited by a high vacuum DC magnetron sputtering system. The Ar pressure was changed from 1.0 to 5.0 mTorr with an interval of 1.0 mTorr during the deposition process. Electron probe microanalysis and Rutherford backscattering are performed to determine the Ar content incorporated within these multilayers. The results demonstrate that less Ar is incorporated within the sample when more Ar is used in the plasma, which could be explained by the increase of the collision probability and the decrease in the kinetic energy of Ar ions arriving at the substrate when more Ar exists. The grazing incident X-ray reflectivity (GIXR) at 0.154 nm is used to determine the structural parameters of the layers. The results show that the structures of these multilayers prepared at different Ar pressure are very similar and that the interface roughness increases quickly when the Ar pressure is higher than 3.0 mTorr. The measurements of the extreme ultraviolet (EUV) reflectivity indicate that the reflectivity decreases when Ar pressure increases. The fitting results of GIXR and EUV reflectivity curves indicate that with an increase of Ar pressure, the density and decrement of the refractive index are increased for W and decreased for Si, which is mainly due to (1) the decrease in Ar content incorporated within these multilayers which affects their performance and (2) the increase of collision probability for sputtered W and Si, the decrease of their average kinetic energy arriving at the substrate, and thus the loosing of their layers.

Key words: multilayer deposition, working pressure, EPMA, RBS, reflectivity

PACS: 81.15.Cd, 68.55.jd **DOI:** 10.1088/1674-1137/36/9/021

1 Introduction

The optical properties of multilayer structures strongly depend on the achievable level of interface perfection [1–3]. Deviations from atomically smooth and chemically abrupt interfaces, i.e. interface roughness and interface diffuseness, respectively, will markedly reduce the reflection coefficients at the interfaces, thereby reducing the overall reflectance of the multilayer stack. Interface imperfections can result from a variety of material- and/or growth-dependent mechanisms, including the formation of mixed composition amorphous interlayers by diffusion or by mixing due to energetic bombardment during growth, and roughness resulting from surface stress or from low adatom surface mobility [4–8]. W/Si multilayers, which have already been found to have relatively small interface imperfections and good performance up to ~70 keV [3, 9], are the subject of the work described here. Once the material combination is determined, the interface width of a multilayer can be further optimized by selecting

Received 12 December 2011, Revised 18 January 2012
* Supported by National Basic Research Program of China (2011CB922203), National Natural Science Foundation of China (11061130549), National International Cooperation Program between China and Japan (2008DFA01920) and Shanghai Natural Science Foundation (09XD1404000)

1) Corresponding author, E-mail: wangzs@tongji.edu.cn

the optimum deposition parameters that minimize the interfacial roughness and diffuseness. The parameters often considered for the optimization process are background pressure, working gas pressure, target-substrate distance and cathode power.

The background pressure has a strong influence on the stress of multilayers [3, 10, 11], i.e. the stress increases as the background pressure increases, mainly resulting from the reduction in surface mobility due to the impurity of the gas atoms (H, O, etc.) present in the vacuum system during deposition. This change in stress is also associated with increased roughness resulting from an impurity-induced reduction in adatom surface mobility. Target-substrate distance can affect the total movement passage of particles and their residual kinetic energy arriving at the substrate, and thus affects the compactness of layers and the interface diffusion of multilayers [12, 13]. Sputtering power has an influence on the deposition rate and multilayer quality due to affecting the average kinetic energy of particles striking on the substrate [3, 13]. Larger power would be expected to result in increased energy delivered to the film surface by particle bombardment. Sputtering power also has an influence on the stress of single layer or multilayer films [14]. Another parameter playing an important role in preparing a multilayer is the working gas pressure [12, 15]. On one hand, the working gas pressure can maintain a normal and stable glow discharge of cathode, thus producing sputtering particles with a steady speed rate; on the other hand, the working gas pressure can affect the kinetic energy of particles arriving at the substrate, thereby affecting the layer compactness and the interface roughness.

The purpose of this paper is to further investigate how the Ar content incorporated within the W/Si multilayers changes as the Ar pressure changes from 1.0 to 5.0 mTorr during the deposition process and how they influence the performance of these multilayers. W/Si multilayers were prepared by a high vacuum magnetron sputtering system at different Ar pressures. The Ar content within these multilayers was determined by electron probe microanalysis (EPMA) and Rutherford backscattering (RBS), respectively. Their performance was characterized using grazing incident X-ray reflectivity (GIXR) at 0.154 nm to determine the structural parameters of the layers and using extreme ultraviolet (EUV) reflectivity at a near-normal incident angle of 10° to determine their reflectivity as a function of Ar pressure. The relationship between the optical constants of W and Si and Ar pressure was deduced by fitting GIXR and EUV reflectivity curves.

2 Experimental details

2.1 Fabrication of multilayers

The W/Si multilayers were prepared by high vacuum DC magnetron sputtering system with four 100-mm-diameter sputtering sources. Before deposition, the base pressure of the vacuum chamber was typically pumped down to 2.0×10^{-4} Pa. During deposition, ultrahigh pure Ar (99.999%) was used as the working gas, and the sputtering sources work at a constant power mode. The distance between the target and the substrate was 8 cm for both targets - W (99.95% purity) and Si (99.999% purity).

Five W/Si multilayers were deposited onto ultrasmooth polished Si substrates (10 mm×10 mm). Over the series of five samples, the Ar pressure was changed from 1.0 to 5.0 mTorr with an interval of 1.0 mTorr. The period number of each sample is 50 and the structures of these multilayers are very similar.

2.2 Electron probe microanalysis

In EPMA an electron beam of a small size, 30 μm, is focused on the sample and by using an adequate calibration procedure it is possible to estimate the content of the elements present in the sample from intensity measurements. Due to the lack of standards for the quantification of Ar, we used a Cl-bearing mineral (scapolite with the general formula $Na_4Al_3Si_9O_{24}Cl$). Cl is the first element preceding Ar in the periodic table and so we calibrated first with the Cl Kα peak, and then the spectrometer was positioned on the Ar Kα peak. The k-ratios were deduced as [counts/s/nA (Ar Kα measured from the unknown)]/[counts/s/nA (Cl Kα from scapolite)]. The given concentration (wt%) is a good estimate and the relative variation between the samples of the studied series is very good. The experimental method was the same for all the samples: two measurements with 5 and 8 keV electrons; for each electron energy, 10 measurements at the same position, then 10 points by scanning about 9 mm of the sample surface. The electron current was 100 nA.

2.3 Rutherford backscattering spectrum analysis

Rutherford backscattering spectrum (RBS) analysis was performed with a NEC 9SDH-2 tandem accelerator using a double-charged $^4He^+$ beam at an energy of 1.8 MeV and a beam current of ~20 nA.

The ions, backscattered at 165° with respect to the incident direction, were energy analyzed by a standard Au-Si surface barrier detector. The energy calibration of the detecting system was carried out with thin films of pure elements, such as Cu, Ag and Au, on a Si substrate. Three well-separated peaks of these elements were used to determine the system energy resolution. The RBS-measured profiles were fitted by the software SIMNRA [16] to determine the proportion of the different elements incorporated within the W/Si multilayers.

2.4 X-ray reflectivity at 0.154 nm

The grazing incidence X-ray reflectivity was measured just after the preparation of the samples with a high-resolution X-ray diffractometer (BEDE D1) operating at Cu Kα line (λ=0.154 nm) with the θ-2θ mode. The angular resolution is 0.007°. The grazing incident angle was scanned from 0°–8° with a step of 0.01° in this measurement. The reflectivity curves were fitted using a custom fitting routine called GAXFIT to determine layer thicknesses and interface parameters. The algorithm in GAXFIT is based on a genetic algorithm. This yielded reliable global solutions for the individual layer parameters in the multilayer.

2.5 EUV reflectivity

The EUV reflectivity curves were measured using a high-precision reflectometer on the beamline U27 at National Synchrotron Radiation, Hefei, China. A 600 line mm^{-1} grating was used to select the target wavelength range. A silicon filter was inserted in the beam path to suppress the higher-order harmonics. The incident beam spot was confined by a small hole with a diameter of 3.0 mm. The wavelength-scan measurements were performed at the fixed incident angle of 10°, i.e. near-normal configuration. Two positions on each mirror were measured with an interval of 2 mm near the center.

3 Results and discussion

3.1 EPMA analysis

Due to the high cross section of the gas ions for neutralization and backscattering by the heavier atoms of the sputtering target material, a flux of energetic Ar neutrals arrives at the substrate and is incident on the growing layer. Fig. 1 shows the Ar concentration (wt%) as a function of Ar pressure and for two used incident electron energies (5.0 and 8.0 keV, respectively). The statistical error (standard deviation) is smaller than the size of the points. The two determinations of the Ar content with the two electron energies are consistent. This means that the electron beam does not reach the Si substrate in both cases and that the distribution of Ar is uniform in depth. It is observed that the higher the Ar pressure during the deposition, the lower the Ar content incorporated within the multilayers. The Ar concentration decreases by a factor of 3.3 when the Ar pressure increases from 1.0 to 5.0 mTorr.

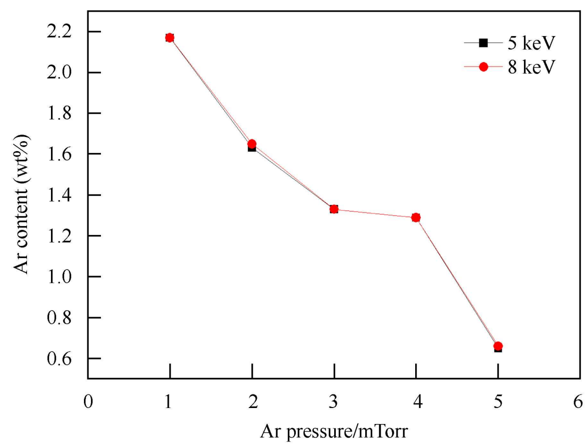

Fig. 1. The evolution of Ar content (wt%) as a function of the Ar pressure and for two used incident electron energies. Each value results from the mean of 10 measurements.

The result can be explained as follows: As the Ar pressure increases, the Ar concentration in the vacuum chamber increases, resulting in the backscattering yield of Ar increasing; however, in addition, the mean free path of gas molecules decreases and in the meantime the probability of collision for the backscattered Ar neutrals is increased. The average kinetic energy of the backscattered Ar neutrals is decreased and their direction of motion changes by collisions with identical mass atoms. This results in slowing down the Ar neutrals and reducing their flux at the substrate and thus the Ar content incorporated within the multilayer is lowered.

As a function of the position on the sample surface no significant change is observed except in case of the sample prepared at 1.0 mTorr where the Ar concentration changes from 2.15 wt% to 2.32 wt% from one edge to the other. This might be caused by the thickness nonuniformity of the multilayer.

3.2 RBS analysis

To further investigate the Ar content incorporated within these W/Si multilayers prepared at different Ar pressure, RBS analysis was performed. Fig. 2

presents the typical RBS spectrum of the five samples prepared at 1.0, 2.0, 3.0, 4.0 and 5.0 mTorr, respectively, measured with $^4He^+$ particles of 1.8 MeV. The arrows indicate the respective energy of the detected He ions for the W, Ar, Si and Si substrates, and Ar (<5.2 at.%) mainly comes from some Ar ions backscattered by target materials during the deposition process. By fitting these RBS profiles, the Ar concentration incorporated within each W/Si sample was determined. Fig. 3 shows the Ar concentration (at.%) as a function of Ar pressure. The same change with pressure as with EPMA measurements is observed, i.e. the Ar proportion decreases as the Ar pressure increases. The reasons for this are discussed in detail in sub-section 3.1.

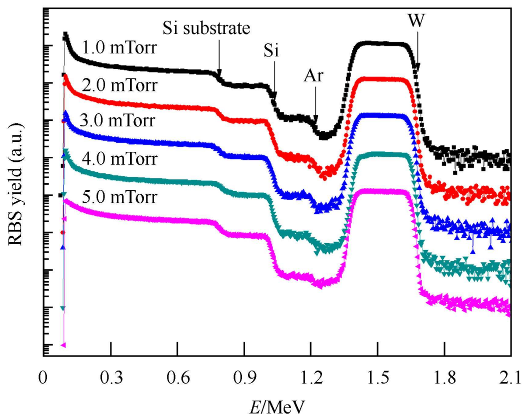

Fig. 2. The RBS spectrum of W/Si multilayers prepared at different Ar pressure obtained with 1.8 MeV $^4He^+$ ions. The arrows indicate the surface energy for W, Ar, Si and the Si substrate.

According to the Ar, W and Si atom percentage (at.%) incorporated within the sample, the weight percentage (wt%) of Ar can be deduced by the formula $A_{Ar}\times a/(A_{Ar}\times a+A_W\times b+A_{Si}\times c)$, where A_{Ar}, A_W, A_{Si} represent the atomic weight of Ar, W and Si, respectively, and a, b, c corresponds to their atom percentage (at.%). With the Ar pressure changing from 1.0 mTorr to 5.0 mTorr, the atom percentage of Ar, W and Si measured by RBS and their corresponding weight percentage are listed in Table 1. These results measured by RBS have an error of ±5.0%. The systematic difference observed between the concentrations determined by RBS and EPMA is very probably due to the fact that in EPMA the concentrations have been estimated from a model considering homogeneous samples and not the multilayer structure of the stacks.

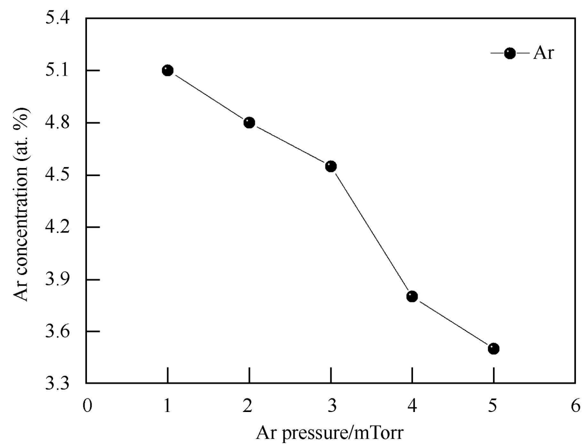

Fig. 3. Ar concentration (at.%) incorporated within the W/Si multilayers versus the Ar pressure.

3.3 X-ray reflectivity at 0.154 nm

The experimental results of X-ray reflectivity of these five multilayers for Cu Kα are plotted in Fig. 4 against the grazing incident angle. The fitted result of each reflectivity curve is also plotted accordingly. The multilayer structural parameters are listed in Table 2.

In Fig. 4, 11 Bragg peaks can be observed in the reflectivity curves of samples prepared at 1.0, 2.0 and 3.0 mTorr, respectively, 8 can be observed for 4.0 mTorr, and only 6 can be observed for 5.0 mTorr, indicating that the multilayer quality of the sample prepared at 5.0 mTorr is the worst and then that prepared at 4.0 mTorr. The fitted parameters listed

Table 1. The Ar, W and Si concentration incorporated within the multilayer prepared at different Ar pressures as determined from RBS measurements.

Ar pressure/mTorr	Ar concentration		W concentration		Si concentration	
	at.%	wt%	at.%	wt%	at.%	wt%
1.0	5.1±0.26	2.68	33.35±1.67	72.13	61.55±3.08	25.19
2.0	4.8±0.24	2.53	33.2±1.66	72.02	62.0±3.1	25.45
3.0	4.55±0.23	2.39	33.5±1.67	72.31	61.95±3.1	25.30
4.0	3.8±0.19	2.01	33.2±1.66	72.11	63.0±3.15	25.89
5.0	3.5±0.18	1.73	37.1±1.85	75.37	59.4±2.97	22.89

Table 2. Structural parameters of each W/Si multilayer sample.

Ar pressure/mTorr	d_W/nm	d_Si/nm	σ (W-on-Si)/nm	σ (Si-on-W)/nm
1.0	2.28	4.60	0.38	0.27
2.0	2.20	4.53	0.38	0.27
3.0	2.18	4.58	0.39	0.28
4.0	2.18	4.51	0.49	0.32
5.0	2.42	4.12	0.51	0.41

in Table 2 can serve to illustrate the above results. The interface roughness (σ) increases quickly at both W-on-Si and Si-on-W interfaces when the Ar pressure is higher than 3.0 mTorr. This can be explained by the increasing collision probability with increasing Ar pressure, as the average kinetic energy of the sputtered atoms is decreased and thus the surface mobility of the adatoms is decreased, resulting in the layer being loosened, the interface width increased, the specular reflectivity reduced and the multilayer quality deteriorated. The slight asymmetry of the W-on-Si and Si-on-W interlayers is mainly due to the mixing resulting from energetic bombardment [3, 17].

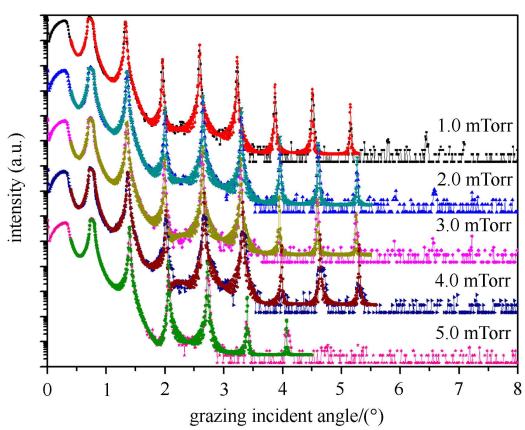

Fig. 4. Grazing incident X-ray reflectivity at 0.154 nm, measured and fitted, for five W/Si multilayer samples.

By fitting these GIXR curves, the density of W or Si also can be determined. As shown in Fig. 5, the density change for W increases from 90% to 93%, while that for Si decreases from 107% to 96%, with the increase of Ar pressure. This is mainly due to two reasons: (1) Ar content decreases with Ar pressure increasing and thus the effect of Ar decreases accordingly, resulting in the density of W and Si approaching their bulk value. (2) the number of Ar atoms increases in the vacuum chamber with Ar pressure increasing, resulting in the decrease of the mean free path of gas molecules and the increase of the collision probability for sputtered particles prior to arrival at the substrate. Due to the collisions increasing, the average kinetic energy of Ar atoms which are not ionized increases while that of the backscattered Ar^+ ions and sputtered W and Si atoms decreases, resulting in their layers loosened and their density decreased. Affected jointly by these two reasons, the density of W increases slowly (from 90% to 93%) while that of Si decreases quickly from 107% to 96%.

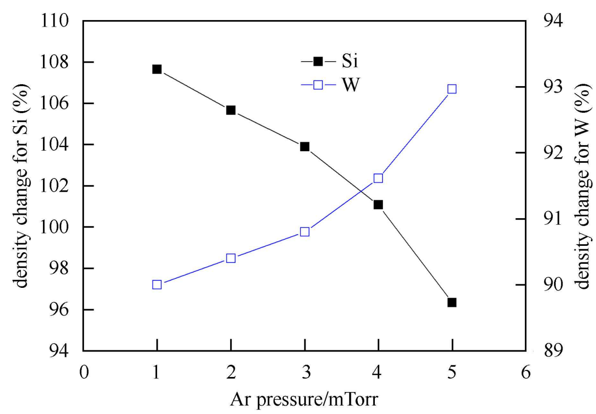

Fig. 5. Density changes of W and Si comparing with their bulk values (100%).

3.4 EUV reflectivity

To further characterize the performance of these multilayers prepared at different Ar pressures, the near-normal incidence EUV reflectance measurements are carried out. Fig. 6 shows the reflectivity curves of four samples prepared at 1.0, 2.0, 3.0 and 4.0 mTorr, respectively, and their corresponding fitting curves. The peak reflectivity is 34.0%, 34.4%, 33.8% and 32.7%, respectively, for the above four samples in the series. The result demonstrates that with Ar pressure increasing by more than 2.0 mTorr, the reflectivity of the W/Si multilayer decreases accordingly, mainly due to the decrease of the surface mobility of adatoms and the increase of the interface roughness with increasing Ar pressure. The peak shift is mainly due to the difference of layer thickness among these samples.

By fitting these EUV reflectivity curves, the change of the decrement of the refractive index δ for W and Si with Ar pressure can be determined, shown in Fig. 7. The change trend for W or Si is almost the same as that of the density shown in Fig. 5, i.e. the change in the decrement of the refractive index for

W increases while that of Si decreases with the Ar pressure increasing, and both tend to for their bulk values, which also might be caused by the Ar content within the W/Si multilayers prepared at different Ar pressure.

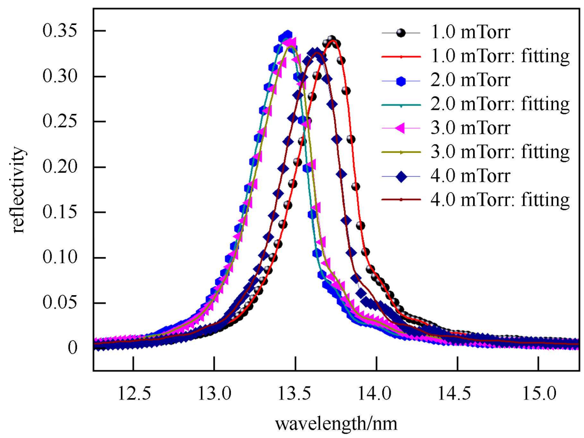

Fig. 6. EUV reflectivity curves of samples prepared at 1.0, 2.0, 3.0 and 4.0 mTorr, respectively, and their corresponding fitting results.

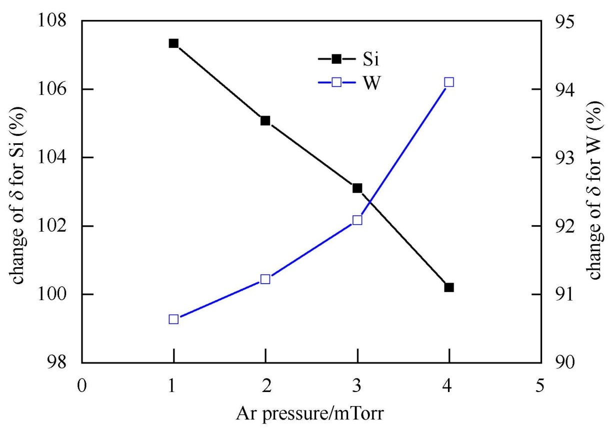

Fig. 7. Change in the decrement of the refractive index for both W and Si compared with their bulk values (100%) versus the Ar pressure.

4 Conclusion

The W/Si multilayers were deposited at different Ar pressures using a high vacuum DC magnetron sputtering system. Their performance is characterized by grazing incidence X-ray reflectance measurement and by near-normal incidence EUV reflectance measurement. The Ar content incorporated within the multilayer is measured by electron probe microanalysis and Rutherford backscattering analysis. Grazing incident X-ray reflectivity measurements at 0.154 nm show that the number of Bragg peaks observed in the reflectivity curves decreases with increasing Ar pressure and that only six Bragg peaks are observed at 5.0 mTorr, indicating that the multilayer quality deteriorates with increasing Ar pressure, mainly due to the increase of interface roughness caused by the low energy of the sputtered atoms after many collisions with the Ar gas. EUV reflectivity measurements show that the peak reflectivity decreases as Ar pressure increases. By fitting the GIXR and EUV reflectivity curves, the change in the trend of the optical constant of W or Si with Ar pressure is determined, i.e. the decrement of the refractive index for W increases while that of Si decreases with increasing Ar pressure, and both tend to do the same for their bulk values. The results obtained by EPMA and RBS show the same changes in Ar concentration with pressure, i.e. the higher the Ar pressure during the deposition, the lower the Ar content incorporated within the multilayers, which might result in the change of the W and Si optical constants. The increase of the collision probability and the decrease of kinetic energy of Ar ions should account for these results.

References

1 Stearns D G. J. Appl. Phys., 1989, **65**(2): 491–506
2 Windt D L, Waskiewicz W K, Griffith J E. Appl. Opt., 1994, **33**(10): 2025–2031
3 Windt D L, Christensen F E, Craig W W et al. J. Appl. Phys., 2000, **88**(1): 460–470
4 Birch J, Eriksson F, Johansson G A et al. Vacuum, 2002, **68**(3): 275–282
5 Petford-Long A K, Stearns M B, CHANG C H et al. J. Appl. Phys., 1987, **61**(8): 1422–1428
6 Rosen R S, Stearns D G, Viliardos M A et al. Appl. Opt., 1993, **32**(34): 6975–6980
7 Bhattacharyya D, Poswal A K, Senthilkumar M et al. Appl. Surf. Sci., 2003, **214**(1): 259–271
8 WANG Y, ZHOU H, ZHOU L et al. J. Appl. Phys., 2007, **101**(2): 023503
9 Madsen K K, Christensen F E, Jensen C P et al. Proc. SPIE, 2004, **5168**: 41–52
10 Windt D L, Brown W L, Volkert C A et al. J. Appl. Phys., 1995, **78**(4): 2423–2430
11 Mirkarimi P B. Opt. Eng., 1999, **38**(7): 1246–1259
12 Ivan A, Bruni R, Byun K, et al. Proc. SPIE, 1999, **3773**: 107–112
13 Berendse F, Owens S M, Serlemitsos P J et al. Appl. Opt., 2003, **42**(10): 1856–1866
14 Tinone M C K, Haga T, Kinoshita H. J. Electron. Spectrosc. Relat. Phenom., 1996, **80**: 461–464
15 Fullerton E E, Pearson J, Sowers C H et al. Phys. Rev. B, 1993, **48**(23): 17432–17444
16 http://home.rzg.mpg.de/∼mam/
17 Hasan M M, Highmore R J, Somekh R E. Vacuum, 1992, **43**(1-2): 55–59